Mechanisms of Peroxynitrous Acid and Methyl Peroxynitrite, ROONO (R = H, Me), Rearrangements: A Conformation-Dependent Homolytic Dissociation

Yilei Zhao,[†] K. N. Houk,*[,†] and Leif P. Olson[‡]

Department of Chemistry and Biochemistry, University of California, Los Angeles, California 90095-1569, and Eastman Kodak Company, 1999 Lake Avenue, Rochester, New York 14650-2102

Received: March 26, 2004

The O−O bond breaking reactions of peroxynitrous acid and methyl peroxynitrite, ROONO (R = H, Me), were investigated theoretically using the (U)CCSD/6-31+G*, (U)CCSD(T)/6-31+G*//(U)CCSD/6-31+G*, and CBS-QB3 methods. The OONO dihedral angle has a remarkably large influence on the barriers for cleavage of the O−O bonds, which influences the subsequent radical recombination to yield nitrates ($RONO_2$). A barrier of ca. 18−19 kcal/mol is predicted for RO−ONO dissociation involving a $^2A_1$-like NO_2 fragment in transition states beginning from a *cis*-OONO conformation. This pathway is significantly favored relative to a $^2B_2$-like transition state with a *trans*-ONOO conformation; the latter has a barrier of 33−34 kcal/mol. Notably, the favored *cis*-OONO pathway is "electronically correct" (because $^2A_1$ NO_2 is a N-centered radical), but "geometrically incorrect" for subsequent N−O bond formation to yield $RONO_2$. The imperfect initial orientation of RO/NO_2 for N−O bond formation rationalizes some escape of free radicals, in competition with low-barrier RO• and NO_2 orientational motions followed by near-barrierless collapse to $RONO_2$. For HOONO, the pathway for $HONO_2$ formation may include a hydrogen-bonded intermediate, •OH···ONO•, earlier proposed as a source of one-electron processes occurring after O−O bond cleavage. The *cis*-ONOO rearrangement barrier is in accord with the experimental free energy of activation (18 ± 1 kcal/mol) for the rearrangement of peroxynitrous acid (HOONO) into nitric acid (HNO_3). MeOONO has a similar rearrangement mechanism, although the pathways for its rearrangement lack any hydrogen-bonded intermediates.

Introduction

Peroxynitrite and related compounds play a very important role in biochemistry and atmospheric chemistry. Peroxynitrite may be formed in vivo from superoxide and nitric oxide.[1] The anion is fairly stable, but the protonated form ($pK_a = 6.8$) decays to nitrate with a rate constant of 0.65 ± 0.5 s^{-1} at 37 °C.[2] The experimental activation parameters for this process are $\Delta H^‡ = 18 \pm 1$ kcal/mol, $\Delta S^‡ = 3 \pm 2$ (cal/mol)/K, and $\Delta G^‡ = 17 \pm 1$ kcal/mol.[3] Oxidations arising from HOONO involve both one- and two-electron processes.[4] It has been proposed that the intermediates (HO• and NO_2•) formed in the HOONO → $HONO_2$ rearrangement reaction may participate in one-electron oxidative reactions.[5] The formation of hydroxyl radical from peroxynitrous acid is still disputable according to the studies by Koppenol and co-workers.[6] In the atmosphere organic peroxyl radicals, ROO•, combine with nitric oxide, an NO_x species formed photochemically in smog and also found in automobile exhaust.[7] Subsequent rearrangement of the ROONO formed in this way is an important reaction that yields alkyl nitrates, $RONO_2$.[8] An intermediate of the rearrangement, NO_2•, leads to tropospheric ozone formation.[9] Among the motivations to understand the mechanism of rearrangement is that it may help to evaluate the hypotheses that air traffic in the upper troposphere leads to substantial increases in tropospheric ozone levels.

Using density functional theory (DFT), the enthalpy of O−O bond dissociation in HOONO to NO_2• and HO• has been calculated as only 19.7 (CBS-QB3) or 22.5 (B3LYP/6-31G*) kcal/mol, while the free energy for this homolysis is only 9.0 kcal/mol.[5] These calculations also suggested that O−O bond homolysis in HOONO leads to either of two structurally similar hydrogen-bonded radical pairs (Figure 1). Both the *endo*- and *exo*-intermediates are stabilized by 2 kcal/mol, relative to free NO_2• and HO• radicals. Recombination of these nascent "caged" radicals to form nitric acid is barrierless, except for the 2 kcal/mol necessary to break the hydrogen bonds. Therefore, O−O cleavage is the rate-determining step for HOONO rearrangement.

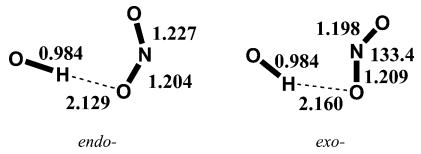

Figure 1. Calculated intermediate complexes of homolysis of HOONO.[5]

However, the detailed mechanism of the O−O cleavage is still an open question. Of particular interest has been the involvement (or lack thereof) of discrete RO• and NO_2• radical intermediates. Even though an experimental free energy of activation, +17 kcal/mol, for peroxynitrite was measured and most reported observations support the homolysis of HOONO into OH• and NO_2•, the mechanism of this transformation has been heavily debated.[1,3] In recent years, transition structures corresponding to O−O cleavage from the *trans*-conformation have been characterized at the MP4SDQ,[10] B3LYP,[11] and CASSCF(8,8)[12] levels. These calculations typically predict that the concerted mechanism has an activation energy of 47−60 kcal/mol.[13] If true, this cannot be a contributing pathway in the HOONO−$HONO_2$ conversion.

[†] University of California.
[‡] Eastman Kodak Co.

10.1021/jp048661w CCC: $27.50
Published on Web 06/16/2004

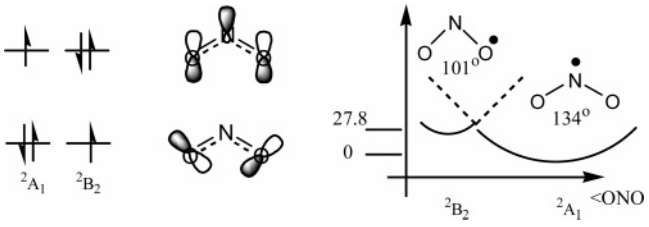

Figure 2. Orbital occupation of the ground ($^2A_1$) and excited ($^2B_2$) states of NO_2. (The $^2B_2$ state, with a smaller ONO angle, is 27.8 kcal/mol higher in energy than the ground state.)

It has been reported that the reaction between MeOO• and •NO is very fast, with a barrier of only 1.2 ± 0.3 kcal/mol, but no direct $MeONO_2$ product was detected if MeO• radicals are scavenged by a high concentration of O_2.[14] This suggests that a concerted rearrangement is not achievable at room temperature and 100 Torr of pressure. Smog chamber studies show that organic nitrates do begin to form as the size of the alkyl group increases.[15] Until recently, computational efforts to find a low-energy pathway for the ROONO unimolecular isomerization, like that of HOONO, have also failed.[16]

In a recent CBS-QB3 study of the unusual NO_2 dimer species ONOONO,[18] we reported the phenomenon of conformation-dependent state selectivity that strongly influences the energetics of its O−O bond breaking transition states (TSs). The conformational feature of importance is the O−O−N−O dihedral angle. This has a large effect on the O−O bond breaking activation barriers; i.e., that for *trans,perp,trans*-ONOONO is 29.8 kcal/mol, that for *trans,perp,cis*-ONOONO is 13.0 kcal/mol, and that for *cis,perp,cis*-ONOONO is 2.4 kcal/mol. (Similar results were obtained at other theoretical levels besides CBS-QB3.) The *trans,perp,trans*-ONOONO O−O bond breaking activation energy is close to a typical dialkyl peroxide RO−OR BDE of ∼30 kcal/mol, but the presence of one *cis*-OONO moiety lowers the activation energy by 16.8 kcal/mol, and the presence of two such moieties lowers the activation energy by 27.4 kcal/mol. On average, this is about 14 kcal/mol per *cis*-ONOO group.

The reason for this has to do with the X−ONO fragment being formally bound as a (distorted) O-centered radical, similar to the $^2B_2$ electronically excited state of NO_2. The energy gap of $^2A_1$ and $^2B_2$ NO_2 has been reported as ∼17−28 kcal/mol (Figure 2).[19] When the O−O bond breaks, the NO_2 fragment can relax to the ground $^2A_1$ state and recover some of the $^2B_2 \rightarrow {}^2A_1$ potential energy, hence the low BDEs of RO−ONO species (lower than those of simple dialkyl peroxides), when the ROONO starting material is compared to the separated radical pair RO• and (relaxed $^2A_1$) NO_2. Note that this effect is not general to nitrogen oxides; e.g., RO−ONO_2 bond dissociation energies are not similarly lowered, because NO_3 does not have a relaxation pathway of nearly the same magnitude of energy as is available to NO_2.[5b] To the extent that the NO_2 $^2B_2 \rightarrow {}^2A_1$ energy loss is available in the transition state, the activation energy of the O−O bond breakage may be lowered. At least for the ONOONO case, this condition is satisfied only from the *cis*-ONOO conformation, not the *trans*-ONOO conformation.

We reasoned that this *cis*-ONOO effect of lowering the activation barrier by ∼10−17 kcal/mol would not be peculiar to ONOONO but might encompass better known yet related species such as ROONO (R = H, alkyl), discussed herein. In ROONO, such a *cis* effect might easily have been overlooked, inasmuch as the ROONO → $RONO_2$ transformation (whether concerted or stepwise) tends to appear most compatible with the *trans*-OONO conformation as the starting point.

We note that Dixon et al.[17] recently located a very dissociative transition state (RO···N distance 2.784 Å, RO···O distances 3.36 and 3.42 Å) for the HOONO−$HONO_2$ rearrangement, using MP2/cc-PVTZ geometry optimization. This structure (Figure 2 of ref 16) is of some concern with respect to our conformational-preference hypothesis, as the computed activation energy (CCSD(T)/CBS//MP2/cc-PVTZ) is only 21.4 kcal/mol relative to *perp,trans*-HOONO, despite the unfavorable *trans*-ONOO conformation. We note that not only are the HO/NO_2 distances rather long, but also the NO_2 fragment (ONO angle 139.5°) is clearly in the $^2A_1$ electronic state, hence the relatively low energy of the radical pair.

Earlier, we discussed initial findings regarding the *cis*-OONO effect on O−O bond breakage in HOONO.[5b] However, using (U)B3LYP/CBSB7 calculations, we were unable to locate true saddle points for this process. Here, we provide new theoretical evidence for the mechanisms of ROONO dissociation into RO and NO_2 radicals through a low-energy pathway via the *cis*-conformation. We report both reaction energetics and transition states for reactions of interest that may help establish which mechanisms are feasible.

Theoretical Methods

Geometries and energies were calculated with DFT using the (U)B3LYP functional,[20] with the 6-311++G** (for HOONO) or 6-31+G* (for MeOONO) basis set using Gaussian 03.[21] Minima and transition states were fully optimized and characterized by harmonic vibrational frequency analysis. The stationary points were also optimized with the complete basis set (CBS-QB3) methodology, known to provide thermochemical estimates approaching experimental accuracy, and also with a coupled-cluster approximation using single and double substitutions ((U)-CCSD)[22] using Gaussian 03 (only this last version supplies CCSD-level optimization). The stationary points were also reevaluated with the (U)CCSD(T) method based on (U)CCSD-optimized structures. All energetics for minima adopted the results of the CBS-QB3 method, because of its high accuracy for minima.[23] All activation energies were deduced from (U)-CCSD(T) single-point calculation based on (U)CCSD-optimized structures, since it is the highest level calculation in the present work. The energies of the first-order saddle points were also calculated step-by-step manually following the CBS-QB3 methodology.[24] The CBS-QB3 results were consistent with the (U)CCSD(T) calculation, typically within 0∼2 kcal/mol for relative energies.

All calculations were verified at the UB3LYP level using broken-symmetry wave functions (guess = mix) for optimizations and/or to assess the expectation value of the S^2 operator. The ground states, rotational transition states, and products are pure singlet species, $S^2 = 0$. Radical-pair-like species showed typical diradical character, i.e., $S^2 = 1$, and used only the unrestricted method for geometry optimizations. The largest amplitudes of the single and double excitations in the CCSD wave function, another check on the accuracy of the single-determinant assumption, were at most 0.2 for biradicaloid species and were deemed acceptable as less than 0.3 (we thank a reviewer for this suggestion). We note that a recent characterization of HO/NO_2 biradicaloid singlet states[34] used a set of methodologies similar to those used herein (i.e., UB3LYP and UQCISD optimizations, the latter method being well-known as a reasonable facsimile of UCCSD), checked using CASSCF-{12,10} geometry optimizations to test for multireference

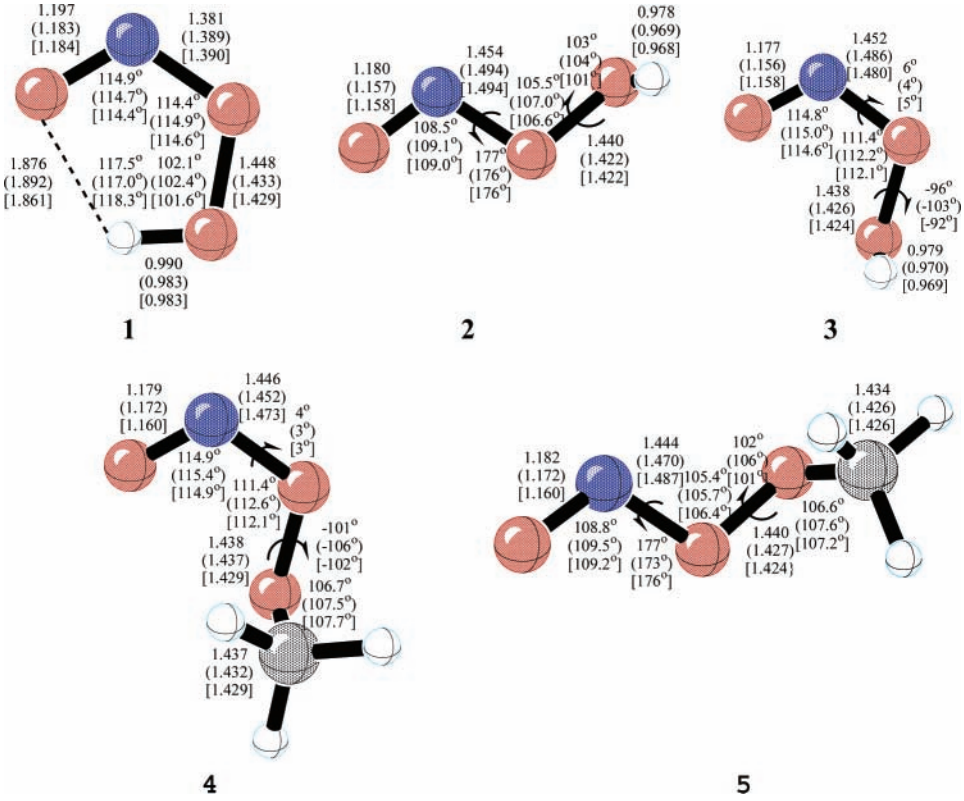

Figure 3. CCSD/6-31+G*-, B3LYP-, and CBS-QB3-optimized structures of *cis*,*cis*-, *trans*,*perp*-, and *cis*,*perp*-conformers of peroxynitrous acid and *cis*,*perp*- and *trans*,*perp*-conformers of methyl peroxynitrite (selected bond lengths in angstroms; angles and dihedral angles are shown).

character. The UB3LYP, UQCISD, and CASSCF results were in agreement with each other, and it was concluded that, for the HO/NO_2 system, unrestricted single-determinant calculations performed well even in cases with spin contamination. (Their calculations are also in accord with ours in other respects, for example, the finding of genuine minima on the HO/NO_2 singlet potential energy surface and the finding that the *cis*-ONOO O−O bond breaking activation energy is quite low: in their case, 12.5−15.7 kcal/mol, depending on the basis set and method).[34]

Another comment concerning the theoretical methods used herein is that although the 6-311++G** and 6-31+G* basis sets are not extremely large (mostly due to the CCSD computational demands), the chief findings of this study have to do with (1) the interesting phenomenon of quite large differences in O−O bond breaking activation energies ($\Delta E_{act} = 17-18$ kcal/mol) between *cis*-OONO and *trans*-ONOO conformations of ROONO and (2) the frankly unsurprising suggestion that reorientations of RO/NO_2 fragments to yield favorable N−O bonding orientations (followed by near-barrierless collapse to $RONO_2$) should be reasonably facile. In neither case would thermochemistry shifts of perhaps a few kilocalories per mole from use of larger basis sets significantly alter the overall mechanistic picture.

Results and Discussion

Conformation of Peroxynitrous Acid and Methyl Peroxynitrite. Structures of peroxynitrous acid have been explored previously using ab initio calculations. Our results agree with earlier calculations.[16,17,25,34] For peroxynitrous acid, the lowest energy conformation is a *cis*,*cis*-conformer with an intramolecular hydrogen bond, **1** (Figure 3). The *trans*,*perp*-conformer **2**, which has the oxygen−hydrogen bond nearly perpendicular to the plane defined by the nitrogen and the oxygen atoms, is 1−3 kcal/mol higher in energy with the B3LYP, CBS-QB3, or CCSD(T) method but 0.5 kcal/mol lower at the CCSD level. The *cis*,*perp*-conformer **3** is the most stable conformation with the CCSD method, 0.4 kcal/mol lower in energy than *cis*,*cis*-conformer **1**, but becomes a little bit higher (0.2−1 kcal/mol) in energy when it is revalued with the CBS-QB3 and CCSD(T) methods. In the case of MeOONO, the *cis*,*perp*-conformer **4** is more stable than the *trans*,*perp*-conformer **5** by about 1.5 kcal/mol. The fluctuation in energy for *cis*,*cis*-conformer **1** with different methods could be argued as due to the competing contribution between O−O lone-pair repulsion and OH···O hydrogen bonding.

The calculated geometrical parameters of *cis*,*cis*- and *trans*,*perp*-conformers of HOONO are quite consistent with the IR vibrational data available from NIST (Table 1). Since a hydrogen bond is present in the *cis*,*cis*-conformer, the vibrational frequencies of the O−H and N═O stretches are red-shifted by 260 and 100 cm^{-1}, respectively, compared to those of the *trans*,*perp*-conformer. A 30 cm^{-1} blue shift for the O−O stretching frequency is associated with a 0.008 Å shorter bond in the *trans*,*perp*-conformer at the CCSD/6-31+G* level.

Transition States for Conformational Isomerization. The isomerizations of peroxynitrous acid (HOONO) have been previously investigated using B3LYP and MP2 methods.[12,27] Here we consider only *cis*/*trans* isomerization of the O−O−N−O moiety, not isomerizations of the H−O−O−N moiety. Both inward and outward rotations around the N−O bond were located, with a barrier of ∼13−15 kcal/mol at the B3LYP/6-311+G** level or ∼9−11 kcal/mol at the MP2/6-311+G** level, with outward rotation favored by about 1 kcal/mol.

The current CBS-QB3 and coupled-cluster results for HOONO and MeOONO are in agreement with earlier reported calculations for HOONO with B3LYP and MP2. The rotation barrier is 10−11 kcal/mol for HOONO and MeOONO. Transition states

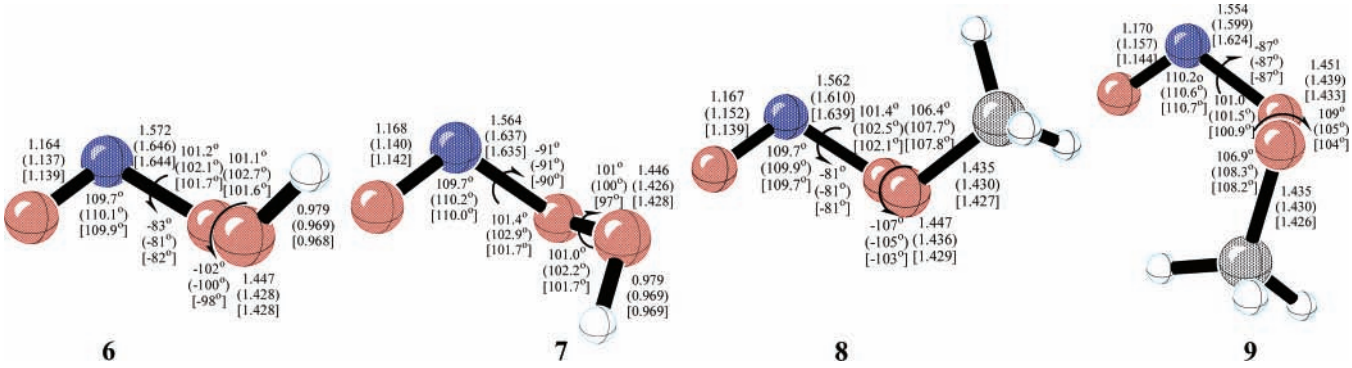

Figure 4. Calculated transition states for the outward and inward isomerization pathways between *cis*- and *trans*-conformers of ROONO (R = H and Me) with the CCSD/6-31+G*, B3LYP, and CBS-QB3 methods (selected bond lengths in angstroms).

TABLE 1: IR Vibrational Data Observed Experimentally and Corresponding Bond Lengths (ca.) of *cis,cis*- and *trans,perp*-HOONO with the CCSD Method

	bond length (Å)	stretching vibration (cm^{-1})	medium	ref 26a−f
		cis,cis-Conformer		
O−H	0.990	3285.4	Ar	a, b
N═O	1.197	1600.3	Ar	a, b
O−O	1.448	927.2	Ar	a, b
N−O	1.381	629.1	Ar	a, b
		trans,perp-Conformer		
O−H	0.978	3545.5	Ar	a, c−f
		3563.3	Ar	a, c−e
		3541.7	N_2	c, d, f
N═O	1.180	1703.6	Ar	a, c−f
		1708.3	Ar	a, c−e
		1701.4	N_2	c, d, f
O−O	1.440	952.0	Ar	a, c−f
		957.4	Ar	a, c−e
		960.5	N_2	c, d, f

SCHEME 1

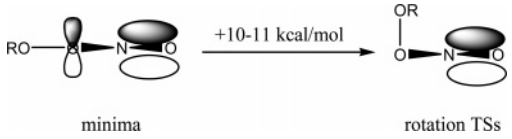

for outward rotation, **6** and **8**, are favored by 1−2 kcal/mol relative to those for inward rotation, **7** and **9** (Figure 4).

Rotational isomerization between *cis*/*trans*-conformers has been found to be rapid at 260−300 K, occurring within 1.5−0.35 ms after formation of HOONO from HO• + NO_2• in a flow chamber.[28] A barrier to rotation is present because the O−N═O fragments in ROONO have some π-conjugation, which may be distorted by a perpendicular orientation of the OR group in a rotational TS, because the conjugated lone-pair electrons are replaced by a π O−O bond (Scheme 1). Near room temperature, gaseous HOONO may exist as a mixture of three the lowest conformers: *cis,cis*-, *cis,perp*-, and *trans,perp*-conformers, with the *cis,cis*-conformer predominating.[28] This would be consistent with observed IR and photodissociation spectra.[29]

O−O Cleavage of Peroxynitrous Acid and Methyl Peroxynitrite. In the absence of oxidizable substrates, peroxynitrous acid decays to nitric acid (k_{obs} = 1.3 s^{-1} at 25 °C).[2] The mechanism for this transformation is problematic. It has been proposed that this is a concerted rearrangement or, alternatively, that it is a dissociative biradical process wherein the activated complex (the intermediate that leads to nitric acid) can also serve as a potent oxidant. In one study, the transition state for the concerted rearrangement of HOONO to HNO_3 was found to lie 60 kcal/mol higher in energy than HOONO (MP4SDQ/6-31G*//HF/6-31G* with SCRF solvation).[10] These authors took the results to support a nonconcerted mechanism. More recent studies[12,17] find transition states either 39.0 kcal/mol (B3LYP/6-311++G**) or 21.6 kcal/mol (MP2/cc-pVTZ) above HOONO for this process, via dissociative pathways that resemble weakly interacting OH• and NO_2• radicals. Because of the dramatic difference in activation energies for O−O bond cleavage reactions in the ONOONO system,[18] we postulated that a transition state arising from the *cis*-OONO conformation would give a lower activation energy as a result of orbital interactions between two separating parts of the RO···ONO radical pair.

In the present work, both *cis*- and *trans*-OONO transition states were located at the UCCSD/6-31+G* level (Figure 5). The transition states are generally diradicaloid, though the degree to which this is true depends on the basis set and method.

The transition states in the *cis*-conformation are lower than

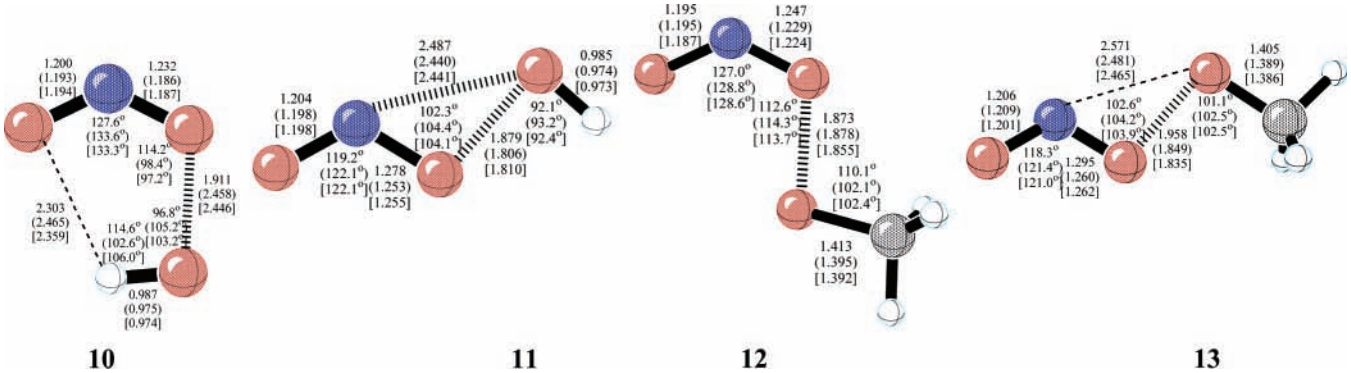

Figure 5. Optimized structures of transition states for O−O cleavage of ROONO (R = H, Me) with the UCCSD, B3LYP, and CBS-QB3 methods (selected bond lengths in angstroms; **10** optimized by the B3LYP/6-311++G** and CBS-QB3 methods results in a 1,3-shift TS).

CHART 1

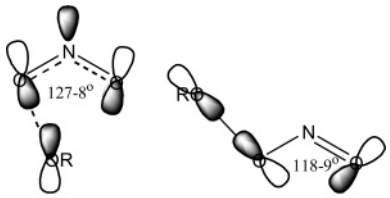

cis- TSs *trans*- TSs

those in the *trans*-conformation, by 17 kcal/mol (UCCSD(T)) for both HOONO and MeOONO. Because the ground-state relative energy of the *trans*-conformer is higher than that of the *cis*-conformer by 1.5−2 kcal/mol (HOONO and MeOONO, respectively, on the basis of the CBS-QB3 method), the activation barrier difference between the *cis*- and *trans*-conformers becomes a bit smaller, e.g., 15 kcal/mol (UCCSD(T)). Note the magnitude of this result is similar to what was found previously for each *cis*-ONOO moiety in the ONOONO system.[5] Because the isomerization between *cis*- and *trans*-conformers has a barrier of 10−11 kcal/mol, much lower than the barrier of O−O cleavage in the *trans*-conformation, the *trans,perp*-ROONO will rotate around the central N−O bond to yield the *cis*-OONO conformer first and then dissociate in a *cis* fashion.

This startling difference in activation barriers between the two conformations can be attributed to state correlations occurring upon formation of the ONO and OR fragments. In the first excited $^2B_2$ state of ONO, a state with the unpaired electron localized on the two terminal oxygen atoms,[18] the singly occupied MO is largely localized on oxygen atoms in an in-plane orbital that is antisymmetric with respect to the C_2 axis.[5] In the $^2A_1$ state, a state with the unpaired electron largely localized on the center N atom,[19] the SOMO is largely localized on an in-plane orbital on the nitrogen atom.[5] The structures of the *cis*-OONO transition states resemble the $^2A_1$ state of ONO, with a larger ONO angle of 127−128° (UCCSD) and a smaller difference[30] of 0.05 Å (UCCSD) in N−O bond lengths for the two peroxynitrites; the *trans*-OONO transition state more closely resembles the $^2B_2$ state, with a smaller ONO angle of 118−119° (UCCSD) and a larger difference of 0.08−0.09 Å (UCCSD) in N−O bond lengths for both peroxynitrites (Chart 1).

At the UB3LYP level, lengthening the O−O distance into isolated ONO• and OH• radicals is purely uphill in energy. The more accurate UCCSD method indicates that the *cis* transition state is a true first-order saddle point for O−O cleavage of HOONO, with an activation energy of 18−19 kcal/mol, similar to recent findings by Bach et al.[34] The partial O−O bond length of 1.91 Å is in the typical range for single bond breaking, compared with the long O−O distances of 2.4 (O_4-O_3) and 2.8 (O_4-O_1) Å at the B3LYP level. This energy is in excellent agreement with the experimental activation enthalpy of 18 ± 1 kcal/mol. In the case of MeOONO, with both the conventional B3LYP and current CCSD methods, eigenvector analysis of the negative eigenvalue indicates simple O−O cleavage for the *cis* transition state, with similar activation energies. The BDE of the O−O bond in MeOONO is 6.7 kcal/mol (CBS-QB3) lower than that in HOONO.[31]

The Nature of HOONO* and Recombination to HNO_3. Interestingly, our most recent results still suggest that the direct product of the O−O cleavage of HOONO may involve an earlier-proposed hydrogen-bonded complex as an intermediate, i.e., •OH···ONO•.[5,32] An activated species, HOONO*, was proposed even earlier as both an intermediate for the HOONO → $HONO_2$ rearrangement and a powerful one-electron oxidant form of peroxynitrous acid.[3] This species has been invoked frequently in the literature, most recently as a hydrated complex with 1−4 water molecules associated preferentially with the HO fragment.[33,34] It was even thought that HOONO* might be a trappable intermediate in the rearrangement.[1] The energy of HOONO* was estimated at 17 kcal/mol above that of peroxynitrous acid,[1,3] close to either the HOONO → $HONO_2$ activation energy, or what we now know is the energy of the HO/NO_2 radical pair. The structures of *endo*- and *exo*-H-bonded complexes, named according to which lone pair of ONO is involved in hydrogen bonding, have been optimized at the UB3LYP level and also reevaluated as single-point energies using UMP2 and UCCSD(T).[5,32] The hydrogen-bonding energies for the diradical complexes (i.e., relative to the isolated radicals) have been calculated as 1.9 and 2.5 for *endo*- and *exo*-complexes, respectively. In the present work, we reoptimized two complexes with the UCCSD/6-31+G* method and tried to locate transition states for the conformational isomerization between the two complexes and also the recombination to nitric acid. We located two complexes and two rotational transition states, **14**−**17**, involved in these isomerizations at the UB3LYP/6-311++G** level (Figure 6). The *endo*-complex intermediate **14** is the direct product from the *cis* transition state for O−O cleavage, while the *exo*-complex intermediate **15** is involved in the recombination to $HONO_2$. Structures **14** and **15** are connected by the twisting transition state **16**. A diradicaloid planar transition state, **17**, with a long N−O distance of 3.07 Å, was located for recombination to nitric acid with the B3LYP method. We find that structure **17** represents the transition state for **15** → $HONO_2$, although it is reminiscent of Dixon et al.'s dissociative transition state for HOONO → $HONO_2$ isomerization. At the UB3LYP level, all those stationary points are very similar in energy, in a range of 1 kcal/mol lower than the free isolated radical pair HO• and ONO•.

To further study the above stationary points, these structures were reoptimized with the UCCSD/6-31+G* method, resulting in only one stationary point, **15**. At the UCCSD/6-31+G* level, attempts to reoptimize the *endo*-complex **14** gave the *exo*-complex **15** instead. The transition-state structure for radical-pair recombination, **17**, could not be located with the UCCSD method due to geometry convergence problems due to the flat potential energy surface, which is consistent with the requirement of only about 1 kcal/mol in energy found by B3LYP to distort the weak hydrogen bond between the radical pair. (Note that this is also consistent with the above-mentioned comparison of our structure **17** with the dissociative MP2/cc-pVTZ HOONO → $HONO_2$ transition state, which is described as "very difficult to obtain", often an indication of a very flat potential energy surface.) Taken as a whole, these data support the idea that a hydrogen-bonded intermediate formed prior to recombination (especially the *exo*-complex) might be among the species exhibiting the "HOONO*" behavior of one-electron oxidation processes.

For the MeOONO system, without the possibility of forming hydrogen-bonded intermediates as in HOONO, the nascent radical pair of RO• and ONO• should simply collapse into alkyl nitrate directly after O−O cleavage, dependent on collision probability. Stepwise formation of $MeONO_2$ fits the experimental observation of the MeOO/NO reaction.[14] The structures of the final products for HOONO and MeOONO rearrangements, nitric acid and methyl nitrate, are shown in Figure 7.

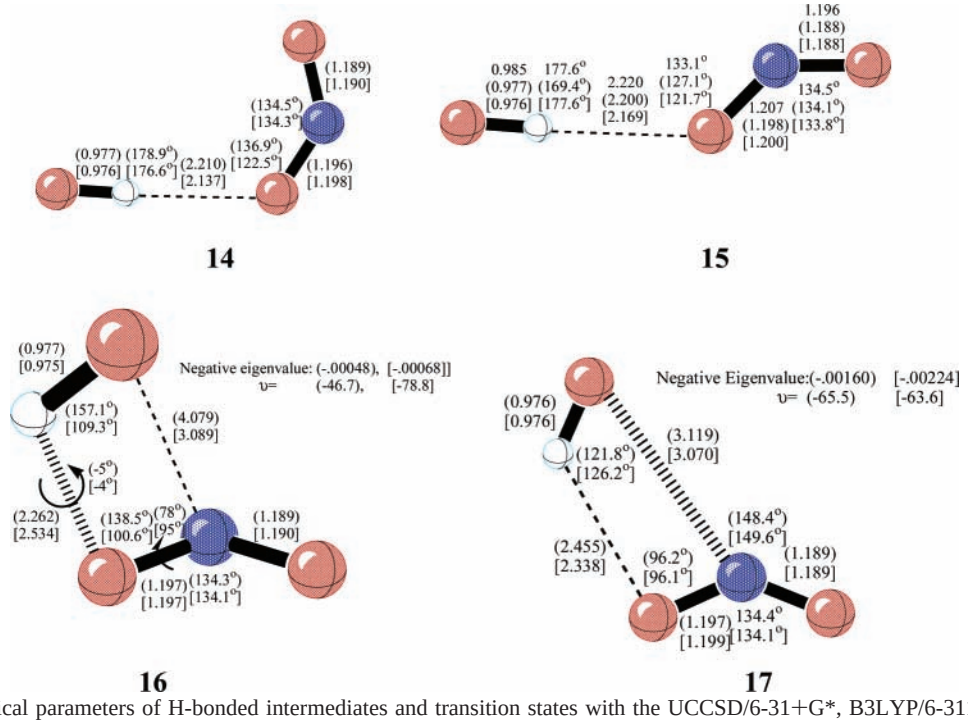

Figure 6. Geometrical parameters of H-bonded intermediates and transition states with the UCCSD/6-31+G*, B3LYP/6-311++G**, and CBS-QB3 methods. (selected bond lengths in angstroms).

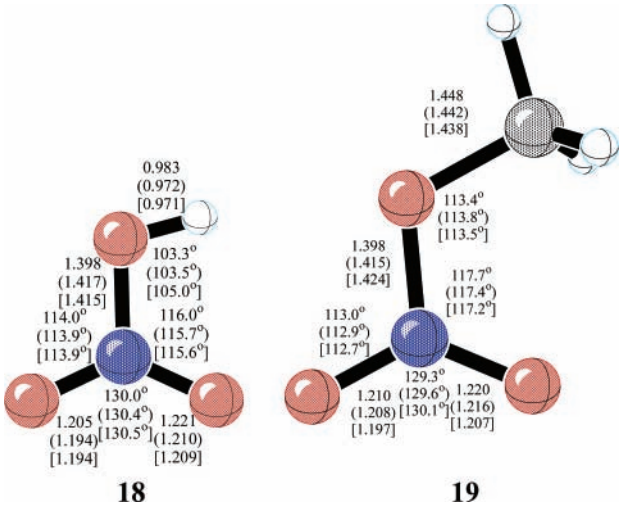

Figure 7. Calculated structures of nitric acid and methyl nitrate with the CCSD, B3LYP, and CBS-QB3 methods.

Conclusions

A summary of all energetic data is shown in Table 2. The energetic profiles for ROONO (R = H and Me) rearrangement to $RONO_2$ are also displayed in Figure 8. For the case of HOONO conversion to nitric acid, the *trans*,*perp*-component in the mixture isomerizes into a *cis*,*cis*-conformer with a barrier of 10 kcal/mol first and then subsequently undergoes O−O cleavage in a low-energy pathway via the *cis*-isomer with a barrier of 18 kcal/mol. The intermediate complexes (•OH···ONO•) may comprise at least part of the HOONO* species taking part in one-electron oxidative processes, along with one-electron oxidations induced by isolated OH and NO_2 radicals that may escape from the hydrogen-bonded radical pair. Although the radical pairs may be oriented in a "geometrically incorrect" fashion for N−O bond formation, they can reorient when necessary and recombine into nitric acid without a significant barrier. The case of MeOONO conversion to methyl nitrate follows a similar pathway. The *trans*,*perp*-conformer first undergoes a slightly exothermic conversion to the *cis*,*perp*-conformer with a barrier of 11 kcal/mol, and then the *cis*-conformer dissociates with a barrier of 19 kcal/mol. The diradical products RO• and ONO• recombine to generate the final product alkyl nitrate exothermically.

In both cases, similar to earlier results with ONOONO,[18] it appears that a *cis*-conformation of the O−O−N−O moiety is the key to a dissociation process that smoothly evolves the NO_2 fragment from the distorted $^2B_2$-like state of the starting material into the lower-energy $^2A_1$ state. The reasons for this have to do with differences in steric effects and orbital overlaps in the *cis*- and *trans*-conformers. The favorable state change results in an O−O dissociation that is lower in activation energy than ordinary O−O bonds (~30 kcal/mol for typical peroxides), e.g., 17−18 kcal/mol for ROONO. The imperfect initial orientation of RO/NO_2 for N−O bond formation rationalizes some escape of free radicals, in competition with low-barrier RO• and NO_2 orientational motions followed by near-barrierless collapse to $RONO_2$.

Understanding O−O bond breaking from the *trans*-conformation is much more troublesome, especially for HOONO, which has hydrogen-bonded radical pairs as stationary points on a flat potential energy surface. Superficially, the *trans*-conformation seems as if it is the best starting point (i.e., "geometrically correct") to accomplish the ROONO → $RONO_2$ isomerization, but it is "electronically incorrect", as activation energies for this process have been reported anywhere from 21.6 to 60 kcal/mol (tending toward much higher activation energies than 21.6 kcal/mol in most cases).[10,11,13,17,20] Much of this broad disparity in energies is probably related to the degree to which the theoretical method (and/or the details of the input geometry) permits the NO_2 radical to resemble the favored $^2A_1$ state. This, in turn, depends on the degree to which the *trans*-OONO transition state in question is a concerted process tending to have a quite high activation energy or resembles two weakly interacting radicals tending to have a lower activation energy (although still higher than that of the *cis* transition state), because the NO_2 fragment is $^2A_1$-like.

It is a difficult question whether a highly dissociative *trans* transition state with a $^2A_1$ NO_2 radical fragment should be

TABLE 2: Calculated Relative Energies for HOONO and MeOONO Conversion to $HONO_2$ and $MeONO_2$ with the B3LYP, (U)CCSD, and CBS-QB3 Methods[a]

	B3LYP /6-311++G**				(U)CCSD	(U)CCSD(T)	CBS-QB3			
	E_{elec}	E	H	G	E_{corr}	E_{corr}	E_{0K}	E	H	G
					HOONO					
1	−14.6	−11.6	−12.2	−1.6	−15.6	−18.0	−18.8	−19.6	−20.1	−9.8
2	−12.5	−9.4	−10.0	+0.2	−15.1	−16.3	−15.9	−16.4	−17.0	−7.2
3	−14.2	−11.2	−11.7	−1.7	−16.0	−17.8	−17.8	−18.3	−18.9	−9.3
6(out)	−1.2	+1.1	+0.5	+11.1	−4.9	−6.3	−6.0	−6.7	−7.3	+2.8
7(in)	−0.3	+2.0	+1.4	+11.9	−4.4	−5.7	−5.5	−6.2	−6.8	+3.3
10(TS)	−2.3	−1.1	−1.7	+7.1	+3.5	+0.4	+1.6	+1.5	+0.9	+9.2
11(TS)	+15.2	+16.2	+15.6	+25.1	+21.8	+17.5	+19.9	+19.5	+18.9	+28.0
14	−1.3	+0.3	−0.3	+4.4	collapse into **15**		−1.3	−0.7	−1.3	+4.0
15	−1.6	+0.0	−0.6	+4.8	−2.1	−1.9	−1.8	−1.2	−1.8	+3.5
16(TS)	−1.3	−0.3	−0.9	+5.3			−2.3	−2.0	−2.6	+3.0
17(TS)	−1.0	+0.0	−0.6	+6.7			+1.4	+1.5	+0.9	+8.4
18	−47.4	−42.8	−43.4	−32.2	−43.9	−45.5	−48.3	−49.4	−50.0	−39.2
					MeOONO					
4	−8.3	−4.7	−5.3	+6.6	−11.9	−14.1	−12.6	−12.8	−13.4	−1.4
5	−7.1	−3.4	−4.0	+8.0	−11.3	−12.9	−11.2	−11.4	−12.0	0.0
8(out)	+5.6	+8.3	+7.7	+20.1	−0.4	−2.1	−0.7	−1.0	−1.6	+10.7
9(in)	+6.4	+9.1	+8.5	+20.9	+0.3	−1.4	−0.1	−0.5	−1.1	+11.3
12(TS)	+2.1	+4.3	+3.7	+14.9	+6.1	+3.0	+7.9	+7.8	+7.2	+18.4
13(TS)	+17.2	+18.7	+18.1	+29.4	+18.2	+19.7	+21.8	+21.8	+21.2	+32.5
19	−39.0	−33.9	−34.5	−21.4	−38.4	−40.0	−42.1	−42.7	−43.3	−30.3

[a] With a reference of free RO and ONO. E_{elec} and E_{corr} are the electronic energies and the energies after coupled-cluster correction, respectively. *E*, *H*, and *G* are the energy involving the ZPE, enthalpy, and Gibbs free energy, respectively. E_{0K} is the energy at 0 K with the CBS-QB3 method.

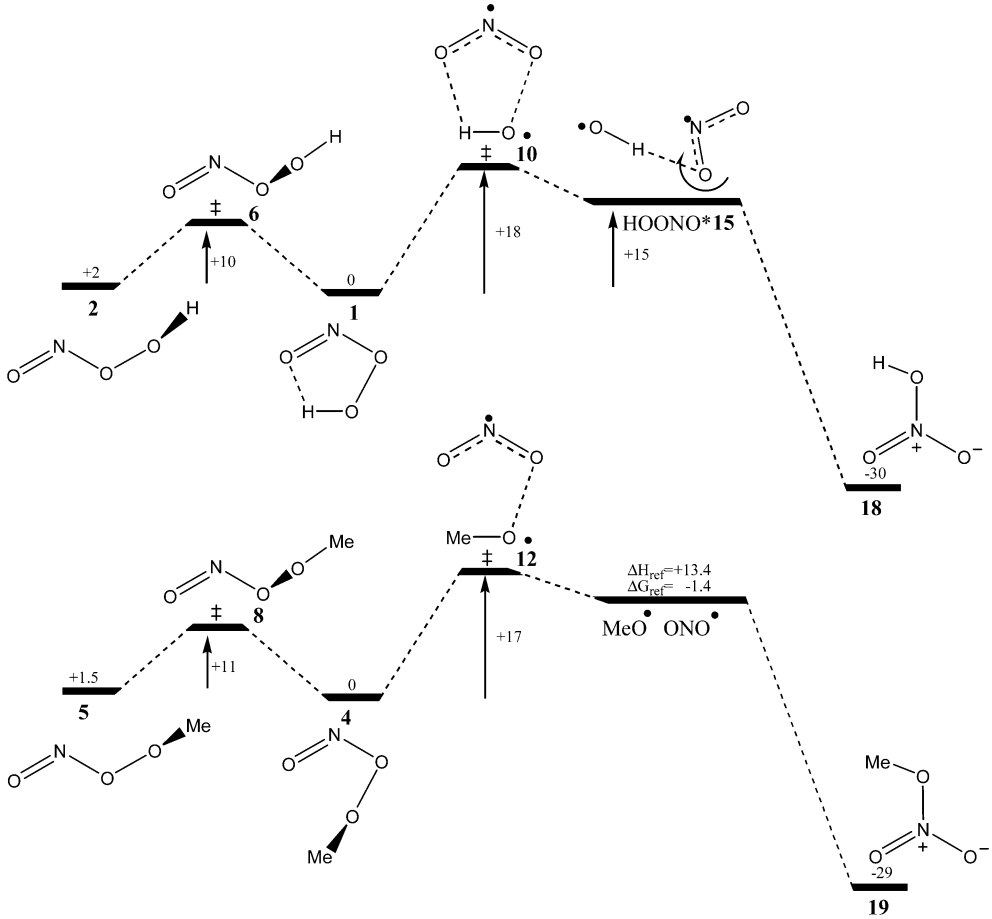

Figure 8. Profiles for HOONO and MeOONO conversion to $HONO_2$ and $MeONO_2$. (Note: Relative energies of minima based on the CBS-QB3 calculation, activation energies of transition states and HOONO* based on the UCCSD(T)/6-31+G*//UCCSD/6-31+G* calculation.)

regarded as real or perhaps simply ill-defined with respect to direct HOONO → $HONO_2$ isomerization. Like structure **17** such a structure exists on a flat energy surface that may simply represent collapse of a preformed radical pair, for example, the conversion of **15** to $HONO_2$.

This has to do with the more complicated issue of whether the vibronically coupled $^2B_2 \rightarrow {}^2A_1$ conical intersection[35] might somehow be accessible from *trans*-OONO conformations, a process possibly not detectable by the present theoretical methods. However, our preliminary CASSCF calculations[36] on the approach of separated HO and $^2A_1$ NO_2 radical pairs indicate that O−O bond breaking from the *trans*-ONOO conformation would receive little or no energy benefit from this conical intersection. In this work, as well as in previous work,[5b] we

have consistently found that RO/NO_2 radical pairs, such as **15** and **14**, are much more readily formed from *cis*-ROONO conformations (as depicted in Figure 8) than from *trans*-ROONO conformations.

Acknowledgment. We are grateful to the National Institute of General Medical Sciences, National Institutes of Health, for financial support of this research, and to NCSA for computational support. We thank Kevin Dockery (EK) for helpful suggestions.

Supporting Information Available: Optimized structures and energies with the (U)B3LYP/CBSB7 (CBS-QB3) and (U)CCSD(T)/6-31+G*//(U)CCSD/6-31+G* methods for all species discussed, and original archive parts in Gaussian calculations (PDF). This material is available free of charge via the Internet at http://pubs.acs.org.

References and Notes

(1) Pryor, W. A.; Squadrito, G. L. *Am. J. Physiol.* (*Lung Cell. Mol. Physiol. 12*) **1995**, *268*, L699−L722.

(2) Beckman, J. S.; Beckman, T. W.; Chen, J.; Marshall, P. M.; Freeman, B. A. *Proc. Natl. Acad. Sci. U.S.A.* **1990**, *87*, 1620.

(3) Koppenol, W. H.; Moreno, J. J.; Pryor, W. A.; Ischiropoulos, H.; Beckman, J. S. *Chem. Res. Toxicol.* **1992**, *5*, 834.

(4) (a) Pryor, W. A.; Jin, X.; Squadrito, G. L. *Proc. Natl. Acad. Sci. U.S.A.* **1994**, *91*, 11173. (b) Padmaja, S.; Squadrito, G. L.; Lemercier, J. N.; Cueto, R.; Pryor, W. A. *Free Radical Biol. Med.* **1996**, *21*, 317.

(5) (a) Houk, K. N.; Condroski, K. R.; Pryor, W. A. *J. Am. Chem. Soc.* **1996**, *118*, 13002 and references therein. (b) Olson, L. P.; Bartberger, M. D.; Houk, K. N. *J. Am. Chem. Soc.* **2003**, *125*, 3999. (c) Similar values were found using high-accuracy coupled-cluster techniques; see ref 17.

(6) Kissner, R.; Nauser, T.; Kurz, C.; Koppenol, W. H. *IUBMB Life* **2003**, *55*, 567 and references therein.

(7) Tyndall, G. S.; Cox, R. A.; Granier, C.; Lesclaux, R.; Moortgat, G. K.; Pilling, M. J.; Ravishankara, A. R.; Wallington, T. J. Atmospheric chemistry of small organic peroxy radicals. *J. Geophys. Res.* **2001**, *106*, 12157.

(8) Ridley, B.; Atlas, E. In *Atmospheric Chemistry and Global Change*; Brasseur, G. P., Orlando, J. J., Tyndall, G. S., Eds.; Oxford University Press: New York, 1999.

(9) Wayne, R. P *Chemistry of Atmospheres*; Oxford University Press: Oxford, U.K., 2000.

(10) Cameron, D. R.; Borrajo, A. M. P.; Bennett, B. M.; Thatcher, G. R. J. *Can. J. Chem.* **1995**, *73*, 1627.

(11) Jursic, B. S.; Klasinc, L.; Pecur, S.; Pryor, W. A. *Nitric Oxide: Biol. Chem.* **1997**, *1*, 494.

(12) Sumathi, R.; Peyerimhoff, S. D. *J. Chem. Phys.* **1997**, *107*, 1872.

(13) While solvation is not identical as in the gas phase, homolysis energetics should not change significantly (see refs 9 and 10).

(14) Scholtens, K. W.; Messer, B. M.; Cappa, C. D.; Elrod, M. J. *J. Phys. Chem. A* **1999**, *103*, 4378.

(15) Arey, J.; Aschmann, S. M.; Kwok, E. S. C.; Atkinson, R. *J. Phys. Chem. A* **2001**, *105*, 1020. Recent research showed that these alkyl nitrate yields are ∼35% lower than previous data reported from the same laboratory in the early 1980s.

(16) Zhang D.; Zhang, R.-Y.; Park, J.; North, S. W. *J. Am. Chem. Soc.* **2002**, *124*, 9600 and previous HOONO calculations (9−12).

(17) Dixon, D. A.; Feller, D.; Zhan, C.-G.; Francisco, J. S. *J. Phys. Chem. A* **2002**, *106*, 3191.

(18) Olson, L. P.; Kuwata, K. T.; Bartberger, M. D.; Houk, K. N. *J. Am. Chem. Soc.* **2002**, *124*, 9469.

(19) (a) Mahapatra, S.; Köppel, H.; Cederbaum, L. S.; Stampfuss, P.; Wenzel, W. *Chem. Phys.* **2000**, *259*, 211. (b) Lievin, J.; Delon, A.; Jost, R. J. *Chem. Phys.* **1998**, *108*, 8931. (c) Blahous, C. P.; Yates, B. F.; Xie, Y.; Schaefer, H. F. *J. Phys. Chem.* **1990**, *93*, 8105. (d) Weaver, A.; Metz, R. B.; Bradforth, S. E.; Neumark, D. M. *J. Chem. Phys.* **1989**, *90*, 2070. (e) Gillispie, G. D.; Khan, A. U.; Wahl, A. C.; Hosteny, R. P.; Krauss, M. *J. Chem. Phys.* **1975**, *63*, 3425. (f) Jaeckels, C. F.; Davidson, E. R. *J. Chem. Phys.* **1976**, *64*, 2908. (g) Jost, R.; Joyeux, M.; Jacon, M. *Chem. Phys.* **2002**, *283*, 17.

(20) Becke, A. D. *J. Chem. Phys.* **1993**, *98*, 5648.

(21) Frisch, M. J.; Trucks, G. W.; Schlegel, H. B.; Scuseria, G. E.; Robb, M. A.; Cheeseman, J. R.; Montgomery, J. A., Jr.; Vreven, T.; Kudin, K. N.; Burant, J. C.; Millam, J. M.; Iyengar, S. S.; Tomasi, J.; Barone, V.; Mennucci, B.; Cossi, M.; Scalmani, G.; Rega, N.; Petersson, G. A.; Nakatsuji, H.; Hada, M.; Ehara, M.; Toyota, K.; Fukuda, R.; Hasegawa, J.; Ishida, M.; Nakajima, T.; Honda, Y.; Kitao, O.; Nakai, H.; Klene, M.; Li, X.; Knox, J. E.; Hratchian, H. P.; Cross, J. B.; Adamo, C.; Jaramillo, J.; Gomperts, R.; Stratmann, R. E.; Yazyev, O.; Austin, A. J.; Cammi, R.; Pomelli, C.; Ochterski, J. W.; Ayala, P. Y.; Morokuma, K.; Voth, G. A.; Salvador, P.; Dannenberg, J. J.; Zakrzewski, V. G.; Dapprich, S.; Daniels, A. D.; Strain, M. C.; Farkas, O.; Malick, D. K.; Rabuck, A. D.; Raghavachari, K.; Foresman, J. B.; Ortiz, J. V.; Cui, Q.; Baboul, A. G.; Clifford, S.; Cioslowski, J.; Stefanov, B. B.; Liu, G.; Liashenko, A.; Piskorz, P.; Komaromi, I.; Martin, R. L.; Fox, D. J.; Keith, T.; Al-Laham, M. A.; Peng, C. Y.; Nanayakkara, A.; Challacombe, M.; Gill, P. M. W.; Johnson, B.; Chen, W.; Wong, M. W.; Gonzalez, C.; Pople, J. A. *Gaussian 03*, revision B.02; Gaussian, Inc.: Pittsburgh, PA, 2003.

(22) (a) Pople, J. A.; Krishnan, R.; Schlegel, H. B.; Binkley, J. S. *Int. J. Quantum Chem. XIV* **1978**, 545. (b) Bartlett, R. J.; Purvis, G. D. *Int. J. Quantum Chem.* **1978**, *14*, 516. (c) Cizek, J. *Adv. Chem. Phys.* **1969**, *14*, 35. (d) Purvis, G. D.; Bartlett, R. J. *J. Chem. Phys.* **1982**, *76*, 1910. (e) Scuseria, G. E.; Janssen, C. L.; Schaefer, H. F., III. *J. Chem. Phys.* **1988**, *89*, 7382. (f) Scuseria, G. E.; Schaefer, H. F., III. *J. Chem. Phys.* **1989**, *90*, 3700.

(23) (a) Montgomery, J. A.; Frisch, M. J.; Ochterski, J. W.; Petersson, G. A. *J. Chem. Phys.* **1999**, *110*, 2822. (b) Petersson, G. A.; Tensfeldt, T. G.; Montgomery, J. A. *J Chem. Phys.* **1991**, *94*, 6091. (c) Ochterski, J. W.; Petersson, G. A.; Montgomery, J. A. *J. Chem. Phys.* **1996**, *104*, 2598. (d) Becke, A. D. *J. Chem. Phys.* **1996**, *104*, 1040.

(24) For the case of saddle points and open-shell species, the CBSB7 basis set is used to obtain geometries in the CBS-QB3 methodology.

(25) (a) McGrath, M. P.; Rowland, F. S. *J. Phys. Chem.* **1994**, *98*, 1061. (b) Tsai, H.-H.; Hamilton, T. P.; Tsai, J.-H. M.; vander Woerd, M.; Harrison, J. G.; Jablonsky, M. J.; Beckman, J. S.; Koppenol, W. H. *J. Phys. Chem.* **1996**, *100*, 15087. (c) Djamaladdin, G. M.; Kirao, K. *J. Phys. Chem. A* **2003**, *107*, 1563.

(26) (a) Lo, W.-J.; Lee, Y.-P. *Chem. Phys. Lett.* **1994**, *229*, 357. (b) Lo, W.-J.; Lee, Y.-P. *J. Chem. Phys.* **1994**, *101*, 5494. (c) Cheng, B.-M.; Lee, J.-W, Lee, Y.-P. *J. Phys. Chem.* **1991**, *95*, 2814. (d) Chen, W.-J.; Lo, W.-J.; Cheng, B.-M.; Lee, Y.-P. *J. Chem. Phys.* **1992**, *97*, 7167. (e) Mielke, Z.; Tokhadze, K. G.; Hulkiewicz, M.; Schriver-Mazzuoli, L.; Schriver, A.; Roux, F. *J. Phys. Chem.* **1995**, *99*, 10498. (f) Koch, T. G.; Sodeau, J. R. *J. Phys. Chem.* **1995**, *99*, 10824.

(27) Jin, H.-W.; Wang, Z.-Z.; Li, Q.-S.; Huang, X.-R. *J. Mol. Struct.: THEOCHEM* **2003**, *624*, 115.

(28) Bean, B. D.; Mollner, A. K.; Nizkorodov, S. A.; Nair, G.; Okumura, M.; Sander, S. P.; Peterson, K. A.; Francisco, J. S. *J. Phys. Chem. A* **2003**, *107*, 6974.

(29) Nizkorodov, S. A.; Wennberg, P. O. *J. Phys. Chem. A* **2002**, *106*, 855. See also ref 25.

(30) Mckee, M. L. *J. Am. Chem. Soc.* **1995**, *117*, 1629. The reverse reaction of NO_2 and X combination requires C_{2v} deformation toward O═N−O. This means the difference between two bond lengths N−O could be considered as somewhat of a reaction coordinate for O−O cleavage.

(31) On the basis of the heats of formation available for HO•, MeO•, NO_2•, HNO_3, and $MeONO_2$ in NIST database, the BDEs of HO−NO_2 and MeO−NO_2 are 49.3 and 41.2 kcal/mol, respectively. Our CBS-QB3 results, 50.0 and 43.3 kcal/mol, are comparable with experimental data.

(32) Musaev, D. G.; Hirao, K. *J. Phys. Chem. A* **2003**, *107*, 1563. See also ref 5.

(33) (a) Pryor, W. A.; Cueto, R.; Jin, X.; Koppenol, W. H.; Ngu-Schwemlein, M.; Squadrito, G. L.; Uppu, P. L.; Uppu, R. M. *Free Radical Biol. Med.* **1995**, *18*, 75. (b) Salgo, M. G.; Stone, K.; Squadrito, G. L.; Battista, J. R.; Pryor, W. A. *Biochem. Biophys. Res. Commun.* **1995**, *210*, 1025. (c) Alvarez, B.; Rubbo, H.; Kirk, M.; Barnes, S.; Freeman, B. A.; Radi, R. *Chem. Res. Toxicol.* **1996**, *9*, 390.

(34) Bach, R. D.; Dmitrenko, O.; Estevez, C. M. *J. Am. Chem. Soc.* **2003**, *125*, 16204.

(35) See, for example: Kirmse, B.; Delon, A.; Jost, R. *J. Chem. Phys.* **1998**, *108*, 6638.

(36) In some of our work in progress, CASSCF[8,8]/6-311G* calculations were done on the approach of separated HO/NO_2 radical pairs, with NO_2 in the $^2A_1$ state. As the O−O distance separating the pair is progressively shortened, the energy rises, for both the *endo* and *exo* cases (e.g., corresponding to *cis*-OONO and *trans*-ONOO dihedral angles, respectively). This is unsurprising, because no X−ONO bond formation is expected from $^2A_1$ NO_2. Importantly, however, the orbital overlaps between the radicals are relatively favorable for the *endo* case and relatively unfavorable for the *exo* case, so the energy rises much more steeply for close O−O approach of HO and $^2A_1$ NO_2 from the *exo* direction. (Inspection of the SOMO of $^2A_1$ NO_2 makes it rather obvious why this might be true.) Further calculations, e.g., different active spaces and basis sets, should be done to confirm this preliminary finding, but it seems consistent with our DFT and coupled-cluster results showing higher energy barriers for O−O bond breaking of ROONO from the *trans*-conformation. That is, if the $^2A_1$ state of NO_2 is reached (e.g., via the $^2B_2 \rightarrow {}^2A_1$ conical intersection) from this conformation, the perturbation due to unfavorable orbital overlaps of the $^2A_1$ NO_2 SOMO with the nearby HO radical eliminates much or all of the energy benefit that would otherwise be expected.